Nonlinear kinematics of a moored axisymmetric wave energy converter

Giuseppe Giorgi*, Josh Davidson†, Giuseppe Habib‡, Giovanni Bracco*, Giuliana Mattiazzo* and Tamas Kalmar-Nagy †

**Department of Mechanical and Aerospace Engineering, Polytechnic of Turin, Turin, Italy*

†Department of Fluid Mechanics, Faculty of Mechanical Engineering, Budapest University of Technology and Economics, Hungary.

‡Department of Applied Mechanics, Faculty of Mechanical Engineering, Budapest University of Technology and Economics, Hungary.

Summary. Mathematical models for wave energy converters (WECs) are naturally germinated from the models in classical offshore engineering applications, where the assumption of linear kinematics and dynamics is commonplace. However, while the assumption of linear, small amplitude, motion fits traditional offshore problems (it is desirable to stabilize ships, boats and offshore platforms), it is not representative of the expected (and desired) motions of a WEC, since the main objective is to enhance the response and maximize power extraction. The inadequacy of linear models for many wave energy applications has led to an increasing number of publications and codes implementing nonlinear hydrodynamics. However, nonlinear kinematics has received little attention, since few models yet consider six degrees of freedom (DoFs) and large rotations. This paper implements a nonlinear kinematic model for one of the most well established WEC concepts: an axisymmetric heaving point absorber with single taut line mooring. The influence of the nonlinear kinematics are demonstrated and potential sources of numerical instability in yaw are discussed. Finally, the model is also used to articulate parametric resonance in roll/pitch.

Introduction

The kinematics and dynamics of floating bodies is traditionally related to offshore engineering problems, such as: naval applications and the design of large oil and gas platforms [1]. For these applications, the main objective is usually to stabilize the motion of the floating objects, therefore the resulting small amplitude motions are within the limits of where linear theory is sufficiently accurate for modelling the system. However, contrary to these conventional offshore applications, wave energy converters (WECs) are designed and controlled with the objective of enhancing the wave induced motion to maximize power absorption [2]. Therefore, it is often the case that linear models become inapt to accurately predict the behaviour of a WEC . The fidelity of mathematical models is crucial for a reliable estimation of the cost of electricity and for the effectiveness of model-based control strategy [3], which are essential for achieving economic viability [4, 5]. Including nonlinearities in energy-maximising control strategies is both essential and possible [6].
As the wave energy field grows in experience and maturity, the necessity of nonlinear models, for a comprehensive design of most WEC types, becomes increasingly apparent [7, 8, 9]. While fully-nonlinear models, such as the ones solving Navier-Stokes equations, achieve high accuracy, they are not computationally viable for control or optimization applications. Considering the more computationally convenient partially-nonlinear models based on potential theory, most of the research is focusing on nonlinear hydrodynamics, namely on the modelling of nonlinear Froude-Krylov, radiation, or diffraction forces, or on viscous effects [10, 11, 12, 13]. However, little effort is found towards modelling nonlinear kinematics [14].
The consideration of nonlinear kinematics is usually necesssary for systems with large amplitude motion and multiple, coupled degrees of freedom. The inclusion of nonlinear kinematics is shown to be important in applications such as biomechanics [15, 16], robotics [17, 18], transportation [19, 20], tracking control [21, 22] and design of manipulators [23, 24], to name a few. However, for wave energy applications, numerical models employed to simulate the dynamic behavious of WECs generally assume the motion to be planar, in the direction of wave travel, with up to 3 DoFs considered (horizontal translation, vertical translation and rotation in the resulting plane: surge, heave and pitch, respectively) [25]. Moreover, the rotational displacement and velocity are normally assumed to be small. Few nonlinear studies are performed in 6-DoFs, especially considering roll/pitch parametric resonance or yaw instability [26, 27]. Parametric resonance is usually detrimental, but the ability to model it can enable more efficient harvesting instead [28, 29].
This paper presents a nonlinear model relevant for wave energy applications, including both nonlinear kinematics and nonlinear hydrodynamics. Typical WEC modelling approaches are challenged, discussing potential issues arising from employing the usual simplifying assumptions. In particular, potential numerical instability may arise from neglecting the mooring line torsional stiffness and viscous dissipation.

Mathematical model for a moored axisymmetric floater

The case study, schematically shown in Figure 1, is the archetype of the popular WEC concept known as a “point absorber” (since its dimensions are small compared to the wavelength such that it can be virtually approximated by a single point). Consequently, a natural choice is to design point absorbers to be independent of the incoming wave direction, so they are normally axisymmetric. The energy extraction results from the relative movement between the buoy and a fixed point on the sea floor. The buoy is attached to the sea floor by a single taut mooring line.

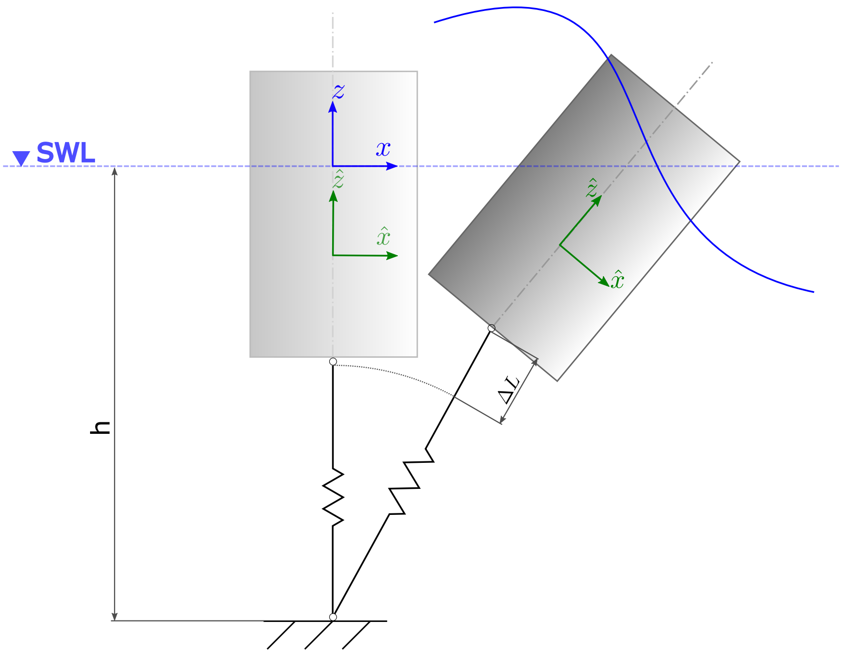

Figure 1: Cylindrical point absorber, with a single taut mooring line tethered to the sea floor (at depth h). Both the inertial frame (x, y, z) and the body-fixed frame $(\hat{x}, \hat{y}, \hat{z})$ have their origin at the still water level (SWL). The floater is shown at rest (in transparency) and displaced. The mooring line has axial stiffness K_{moor}, initial length L_0 and elongation ΔL. The device can rotate with respect to the mooring line.

Reference frames

Two right-handed frames of reference are defined, as schematically shown in Figure 1. The first one (x, y, z) is world-fixed, inertial, with the origin at the still water level (SWL) and on the centre of the buoy at rest, with the $x-$axis along and in the same positive direction of the wave propagation, and the $z-$axis pointing upwards. The inertial frame is used to describe the body displacements ($\boldsymbol{\zeta}$), divided into translations ($\mathbf{p}$) and rotations ($\boldsymbol{\Theta}$):

$$\boldsymbol{\zeta} = \begin{bmatrix} \mathbf{p} \\ \boldsymbol{\Theta} \end{bmatrix} \quad , \quad \mathbf{p} = \begin{bmatrix} x \\ y \\ z \end{bmatrix} \quad , \quad \boldsymbol{\Theta} = \begin{bmatrix} \phi \\ \theta \\ \psi \end{bmatrix}, \tag{1}$$

The second right-handed frame of reference is $(\hat{x}, \hat{y}, \hat{z})$, body-fixed, hence non-inertial, with the origin at the center of gravity of the floater. This is used for writing the dynamic equation of the system, since the inertial matrix remains constant. Therefore, both forces and velocities are represented in the body-fixed frame, along the axis of the buoy. Velocities ($\boldsymbol{\nu}$), divided into translation ($\mathbf{v}$) and rotations ($\boldsymbol{\omega}$), are defined as:

$$\boldsymbol{\nu} = \begin{bmatrix} \mathbf{v} \\ \boldsymbol{\omega} \end{bmatrix} \quad , \quad \mathbf{v} = \begin{bmatrix} u \\ v \\ w \end{bmatrix} = \begin{bmatrix} \dot{\hat{x}} \\ \dot{\hat{y}} \\ \dot{\hat{z}} \end{bmatrix} \quad , \quad \boldsymbol{\omega} = \begin{bmatrix} p \\ q \\ r \end{bmatrix}. \tag{2}$$

Kinematic mapping

It is worth remarking that forces and velocities are along time-varying axes, while displacements are along fixed axes. In linear hydrodynamic models there is no difference between such axes, based on the assumption of small displacements. However, in a nonlinear approach, a mapping from body- to world-frame velocities should be applied, at each time step, in order to obtain the correct displacements. One possible mapping is the following:

$$\dot{\boldsymbol{\zeta}} = \begin{bmatrix} \dot{\mathbf{p}} \\ \dot{\boldsymbol{\Theta}} \end{bmatrix} = \begin{bmatrix} \mathbf{R}_{\boldsymbol{\Theta}} & \mathbf{0}_{3\times3} \\ \mathbf{0}_{3\times3} & \mathbf{T}_{\boldsymbol{\Theta}} \end{bmatrix} \begin{bmatrix} \mathbf{v} \\ \boldsymbol{\omega} \end{bmatrix} = \mathbf{J}_{\boldsymbol{\Theta}} \boldsymbol{\nu}, \tag{3}$$

where $\mathbf{R}_{\boldsymbol{\Theta}}$ is the rotation matrix, depending on the Euler angles $\boldsymbol{\Theta}$, defined according to the 3-2-1 convention as:

$$\mathbf{R}_{\boldsymbol{\Theta}} = \mathbf{R}_{\hat{z},\psi} \mathbf{R}_{\hat{y},\theta} \mathbf{R}_{\hat{x},\phi} = \begin{bmatrix} c\psi & -s\psi & 0 \\ s\psi & c\psi & 0 \\ 0 & 0 & 1 \end{bmatrix} \begin{bmatrix} c\theta & 0 & s\theta \\ 0 & 1 & 0 \\ -s\theta & 0 & c\theta \end{bmatrix} \begin{bmatrix} 1 & 0 & 0 \\ 0 & c\phi & -s\phi \\ 0 & s\phi & c\phi \end{bmatrix}, \tag{4}$$

with c and s standing for $\cos()$ and $\sin()$ trigonometric operators, respectively. $\mathbf{R}_{\Theta}$ is applied to translational velocities. $\mathbf{T}_{\Theta}$ is applied to rotational ones, and is defined as follows:

$$\mathbf{T}_{\Theta} = \begin{bmatrix} 1 & s\phi t\theta & c\phi t\theta \\ 0 & c\phi & -s\phi \\ 0 & s\phi/c\theta & c\phi/c\theta \end{bmatrix}, \tag{5}$$

where t stands for the $\tan()$ trigonometric operator. Note that the singularity of $\mathbf{T}_{\Theta}$ in $\pm\pi/2$ is usually not an issue in wave energy applications, since the amplitude of the pitch angle is, by design, always expected to be smaller than $\pi/2$.

Coriolis and centripetal forces

Another consequence of using a body-fixed frame are Coriolis and centripetal forces, which are normally neglected under the assumption of small rotational velocities. Let us define, for convenience of notation, the skew-symmetric operator $\mathcal{S} : \mathbb{R}^3 \to \mathbb{R}^{3\times3}$ as

$$\mathcal{S} : \left\{ \boldsymbol{\lambda} \in \mathbb{R}^3 \middle| \mathcal{S}(\boldsymbol{\lambda}) \triangleq \begin{bmatrix} 0 & -\lambda_3 & \lambda_2 \\ \lambda_3 & 0 & -\lambda_1 \\ -\lambda_2 & \lambda_1 & 0 \end{bmatrix} \right\}. \tag{6}$$

Using such a notation, it is possible to define Coriolis and centripetal forces as:

$$\mathbf{F}_{Cor} = -\mathbf{C}_{Cor}\boldsymbol{\nu} = -\begin{bmatrix} M\mathcal{S}(\boldsymbol{\omega}) & -M\mathcal{S}(\boldsymbol{\omega})\mathcal{S}(\mathbf{r}_{\boldsymbol{g}}) \\ M\mathcal{S}(\mathbf{r}_{\boldsymbol{g}})\mathcal{S}(\boldsymbol{\omega}) & -\mathcal{S}(\mathbf{I}_r\boldsymbol{\omega}) \end{bmatrix} \begin{bmatrix} \mathbf{v} \\ \boldsymbol{\omega} \end{bmatrix}, \tag{7}$$

where M is the mass of the body, $\mathbf{r}_g$ is the vector from the origin of the body-fixed frame (reference point) to the centre of gravity, and $\mathbf{I}_r$ is the matrix of the moments of inertia with respect to the reference point. If the reference point is coincident with the center of gravity, then $\mathbf{r}_g$ is the null vector and $\mathbf{I}_r$ is a diagonal and minimal matrix, with I_x, I_y, and I_z on the diagonal. Consequently, the Coriolis and centripetal force in (7) becomes:

$$\mathbf{F}_{Cor} = -\begin{bmatrix} M(qw - rv) \\ M(ur - pw) \\ M(pv - qu) \\ qr(I_z - I_y) \\ rp(I_x - I_z) \\ pq(I_y - I_x) \end{bmatrix} \tag{8}$$

Hydrodynamic forces

The wave-structure interaction is modelled using the partially nonlinear hydrodynamic model detailed in [30]. This model decomposes the force from the fluid on the floater into several compoents: the Froude-Krylov (FK) force $\mathbf{F}_{FK}$, the diffraction force $\mathbf{F}_d$, the radiation force $\mathbf{F}_r$ and the viscous force $\mathbf{F}_v$. The model is labelled ”partially nonlinear” since the diffraction and radiation forces are modelled linearly, whereas the viscous and FK force terms are nonlinear. The viscous force is described by an integral quadratic representation, and the nonlinear FK force is calculated by integrating the undisturbed pressure field from the incident wave over the instantaneous (updated at each time step) wetted surface of the floater. Full details of the nonlinear FK force representation are given in [31] for axisymmetric floaters, and in [32] for prismaric floaters. An open-source toolbox for the implementation of the nonlinear FK method is provided in [33].

Mooring force

The mooring system applies a force, $\mathbf{F}_m$, to the attachment point at the bottom center of the floater. The mooring force is modelled here as a linear spring.

Equation of motion

Finally, the dynamical equation in 6 DoFs for the floater becomes:

$$\begin{cases} \dot{\boldsymbol{\zeta}} = \mathbf{J}_{\Theta}\boldsymbol{\nu} \\ \mathbf{M}\dot{\boldsymbol{\nu}} + \mathbf{F}_{Cor} = \mathbf{F}_{FK} + \mathbf{F}_d + \mathbf{F}_r + \mathbf{F}_v + \mathbf{F}_m \end{cases} \tag{9}$$

where $\mathbf{M}$ is the inertial matrix,

Coupling between DoFs

For the case of linear hydrodynamics, incoming unidirectional waves induce a planar external excitation on axisymmetric floaters (surge, heave and pitch). However, when considering nonlinear FK forces, a coupling can manifest under certain conditions, due to an internal excitation of the sway and roll DoFs [31]. In particular, when the excitation frequency is about twice the natural frequency in roll, a Mathieu-type of instability induces parametric resonance [34].
In these regions of parametric instability, a nonlinear FK model can provide 5 DoFs of excitation. Note, there is no means of exciting the yaw DoF. Even when considering the mooring system, the single mooring line does not provide any coupling between the excited DoFs and yaw [35]. However, if nonlinear kinematics effects are introduced, the Coriolis and centripetal forces, as well as the kinematic mapping $\mathbf{J}_{\boldsymbol{\Theta}}$, have the mathematical structure to provide a coupling with yaw. The following sections will show that, if these forces and the kinematic mapping are not appropriately taken into account, then the model can exhibit numerical instability.

Kinematic mapping

The last row of equation (3) represents the mapping from the body-fixed rotational velocities, $\boldsymbol{\omega}$, to the rate of change of the yaw displacement, $\dot{\psi}$:

$$\dot{\psi} = q\frac{\sin\phi}{\cos\theta} + r\frac{\cos\phi}{\cos\theta} \tag{10}$$

If ϕ is not exactly zero, Equation (10) shows that, $\dot{\psi}$ will be greater than zero. For the case of 3-DoF excitation (linear FK model or nonlinear FK model away from the parametric instability region), ϕ is not excited and simply decays from a small initial value ϕ_0; consequently $\dot{\psi} \approx 0$. On the other hand, when 5-DoF excitation occurs (nonlinear FK model in the parametric instability region), roll is internally excited and eventually the term $q\frac{\sin\phi}{\cos\theta}$ is non negligible, nor $\dot{\psi}$ anymore either.
Therefore, it results that the yaw DoF is coupled with other rotational DoFs, either weakly (in the 3-DoF case) or strongly (in the 5-DoF case). However, if there is no excitation of the yaw DoF, the yaw displacement is bounded, since $\dot{\psi}$ is of the same order of magnitude of q: $\dot{\psi} = \mathcal{O}(q)$. Nevertheless, under certain conditions, yaw may also be weakly excited by Coriolis and centripetal forces, potentially inducing the system to be unstable and generate an unbounded yaw response.

Coriolis and centripetal forces

As shown in Equation (8), the surge component of $\mathbf{F}_{Cor}$ is:

$$\mathbf{F}_{Cor}(1) = -M\left(qw - rv\right) \tag{11}$$

It is worth to notice that, in the simple 3-DoF case, the product $rv \approx 0$, so that $\mathbf{F}_{Cor}(1) \approx -Mqw$. Therefore, the mean of $\mathbf{F}_{Cor}(1)$ depends on the phase difference between pitch and heave, which are both externally excited. In particular, a zero mean is obtained if the phase difference is 90°, while strongly negative or positive means are obtained for phase differences of 0 or 180°, respectively. In a linear hydrodynamic model, the surge exciting force has zero mean, so that the resulting surge displacement is bounded to have the same sign of the mean of $\mathbf{F}_{Cor}(1)$, and magnitude depending on the mooring restoring force [35], since no hydrostatic force is present in surge. On the other hand, if a nonlinear hydrodynamic model is used, second order drift effects shift the mean of the surge exciting force to positive values, so that the resulting mean displacement is a combination of both the wave and the Coriolis and centripetal forces.
The yaw component of the $\mathbf{F}_{Cor}$ around the center of gravity, as shown in (8), is the following:

$$\mathbf{F}_{Cor}(6) = -pq\left(I_y - I_x\right) \tag{12}$$

Since pitch is externally excited, q is never zero. Since roll is either internally excited (5-DoF case) or in a simple decay (3-DoF case), p is either significantly large or relatively small, respectively, but never exactly zero. It follows that $\mathbf{F}_{Cor}(6)$ is exactly zero if and only if $I_x = I_y$.

Numerical yaw instability

Generally, both intuition and experience teach that no significant yaw response is expected from an axisymmetric system. Physically, the only restoring force in yaw is provided by moorings. For the mooring system shown in Figure 1, the restoring is provided by the torsional stiffness of the mooring line, which is normally small and usually neglected [36]. Consequently, no yaw restoring term is usually implemented in the numerical model. In addition, no dissipative mechanism are usually implemented in yaw, because radiation damping is ideally zero and viscous losses are reasonably negligible, due to the smooth axisymmetric geometry. However, neglecting dissipative and restoring terms in the yaw DoF can lead to unexpected yaw responses, and potentially generating conditions for numerical instability.

Initial conditions

Let us assume that the initial conditions, ($\boldsymbol{\zeta}_0$), are not exactly zero, but a small fraction of their expected steady state response, so that $\boldsymbol{\zeta}_0$ can be considered 'almost' zero. Such an assumption is consistent with the common application where, a mathematical model is coupled with a physical system, taking measured displacement and/or velocity signals as inputs (either in an experimental test-rig [37] or in real-sea deployment [38]). Furthermore, it is common practice to assume almost-zero initial conditions in nonlinear hydrodynamic models, in order to provide some initial energy to all DoFs and study the effect of instability [39, 40]. In absence of external-internal excitation or strong coupling, the small initial conditions rapidly decay. In the following discussion, the initial roll displacement, (ϕ_0), is slightly greater than zero (say, 0.5°), so that ϕ, $\dot{\phi}$, and p are non-zero.
Furthermore, let us assume that the initial yaw displacement ψ_0 is zero. Although this is an unnecessary assumption, it will highlight that a response in yaw (with no external nor internal hydrodynamic excitation) can appear solely due to the nonlinear kinematics.

Transversal moments of inertia

Theoretically, the two transversal moments of inertia, I_x and I_y, should be identical. However, numerically, the geometrical properties of the buoy will be reproduced with finite accuracy, thus I_x and I_y may be not exactly the same as each other. In this study, as an example, I_y has been considered to be $99.9\% I_x$.

Excitations

Table 1 summarizes all possible conditions that can arise.

Table 1: Characteristic of the yaw oscillatory response, ψ. Considering no viscous nor restoring terms in yaw and a small perturbation of the initial condition in roll and pitch. Two transversal moment of inertia cases are considered: ideal ($I_x = I_y$) and almost-ideal ($I_x \approx I_y$), in combination with two hydrodynamic excitation conditions: 3-DoF (linear FK model or nonlinear FK model away from the parametric resonance region) and 5-DoF (nonlinear FK model close to the parametric resonance region).

	Hydrodynamic excitation	
	3-DoF	**5-DoF**
$I_x = I_y$	Decay	Sustained, $\mathcal{O}(\theta)$
$I_x \approx I_y$	Unstable	Unstable

Let us consider the two hydrodynamic excitation conditions:

- 3-DoF excitation, where the excitation is external only.
- 5-DoF excitation, where 3-DoF are external excitation and 2 DoF are internal excitations present in the nonlinear FK model close to the parametric resonance region.

In the ideal case ($I_x = I_y$), there is no forcing term in yaw, so that the yaw response will follow roll and pitch angles, according to equation (10). In particular, in the 3-DoF excitation condition, yaw will follow the decay of roll; in the 5-DoF excitation condition, the oscillatory part of yaw will follow the pitch sustained response, modulated by the sine of the roll response. A slowly increasing mean of yaw is also present, due to the absence of a restoring force.
However, in the almost-ideal case ($I_x \approx I_y$), equation (12) shows that there is a forcing term of the yaw DoF, much smaller in a 3-DoF scenario than a 5-DoF scenario, but never exactly zero. Consequently, due to the lack of viscous and restoring terms, the yaw DoF is not restrained and becomes unstable, so that its response diverges at a rate proportional to the difference between I_x and I_y. Therefore, when implementing Coriolis and centripetal forces in a 6-DoF model, it is important to include a yaw restoring term, which prevents the numerical instability from appearing.

6-DoF response

A nonlinear 6-DoF model has been implemented, including nonlinear kinematics, Coriolis and centripetal forces, nonlinear Froude-Krylov forces, and 6-DoF quadratic viscous forces, as in [2]. The nonlinear hydrodynamics of this model is able to articulate parametric resonance in roll and pitch, which is a Mathieu-type of instability, arising when the period of the excitation force is about half the natural period in roll and pitch ($T_{n,5}$). Such an instability is mainly induced by the heave displacement causing, among other effects, a time-varying metacentric height (GM), thus hydrodynamic stiffness in roll and pitch.
In order to highlight such a behaviour, the floater, whose schematics is shown in Figure 1, is inspired by the cylinder studied in [41, 42], which is a renown example of parametrically unstable floater, due to the 2:1 ratio between natural periods in pitch/roll and heave. However, a notional single mooring line has been included, in order to consider the full 6-DoF model. For simplicity, the mooring restoring force has been assumed to be linear and with no coupling between DoFs. Note that, in order to avoid numerical instability in yaw, a torsional stiffness of the mooring line has been included. Furthermore, a 0.1% perturbation of one of the two transverse moments of inertia has been considered, in order to highlight the lack of instability thanks to the torsional stiffness.

Finally, note that all parameters and results here presented are normalized, enabling application to structures of varying size, such as the large spars in [41, 42], and to smaller WEC-like structures, as in [43]. The relevant common feature is to realize a 2:1 ratio between pitch and heave natural periods. Table 2 shows the ratio between the natural period in each DoF and $T_{n,5}$.

Table 2: Natural periods normalized by the pitch and roll natural periods [-].

Surge & Sway	**Heave**	**Roll & Pitch**	**Yaw**
7.7	0.5	1	5.1

Figure 2 shows the amplitude of the response to regular waves, as a function of wave periods (T_w) and wave heights (H_w). Periods are normalized by $T_{n,5}$, while the wave height and linear displacements are normalized by the metacentric height (GM). The dashed and dash-dotted red lines correspond to $T_w = \frac{1}{2}T_{n,5}$ and $T_w = T_{n,5}$, respectively. As expected, a roll and sway response is localized around an excitation period equal to $\frac{1}{2}T_{n,5}$. At the same period, there is a clear reduction of heave response, due to an internal exchange of energy between DoFs. Finally, under the 5-DoF excitation condition, there is a small response in the yaw DoF, made possible by the nonlinear kinematics and the perturbation of the transverse moment of inertia. However, due to the restoring term in yaw, numerical instability is avoided and the yaw response is contained below 1 degree.

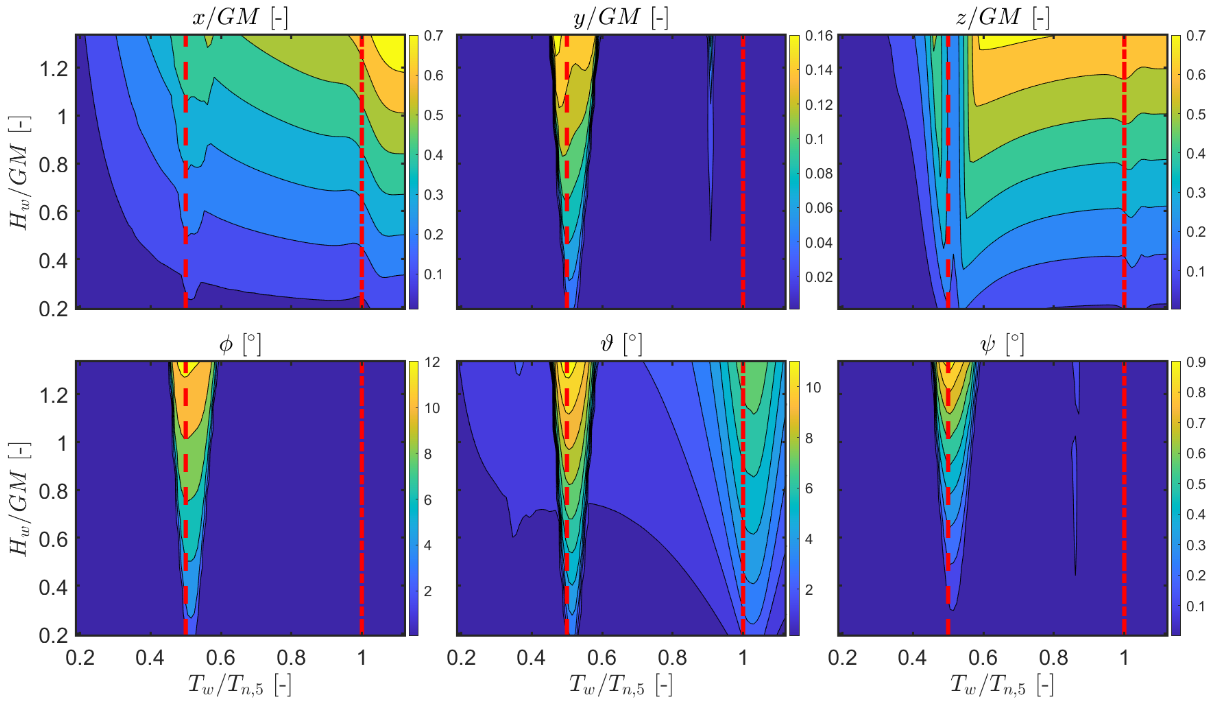

Figure 2: Amplitude of the response as a function of T_w and H_w. Periods are normalized by $T_{n,5}$, while the wave height and linear displacements are normalized by the metacentric height GM. The dashed and dash-dotted red lines correspond to $T_w = \frac{1}{2}T_{n,5}$ and $T_w = T_{n,5}$, respectively.

While Fig. 2 is obtained with a regular (monochromatic) waves, it is interesting to verify the development of parametric resonance and dynamic instability to more realistic irregular (panchromatic) waves. The most interesting condition is at the parametric resonance period, so that a peak period (T_p) of half $T_{n,5}$ is considered. Since the severity of the instability is proportional to the significant wave height (H_s) a medium-high value is considered, based on Fig.2, equal to GM. A typical Jonswap spectrum is considered, with the enhancing factor (γ) of 3.3. Figure 3 shows the dynamic response of the floater for a long realization of the resulting stochastic process. It is clear that the parametric resonance in roll is excited, but reaching a lower steady state amplitude than in the monochromatic condition, since the frequency-dependent instability is weaker.

Conclusions

This paper proposes a model in 6 degrees of freedom for axisymmetric floaters, including nonlinear kinematics, Coriolis and centripetal forces, and nonlinear Froude-Krylov forces. Although their physical impact is negligible, it is crucial to include damping and restoring terms in the yaw degree of freedom in the numerical model. In fact, if yaw is unrestrained, unstable and unbounded yaw responses may appear if there is a perturbation of the inertial properties of the system (likely

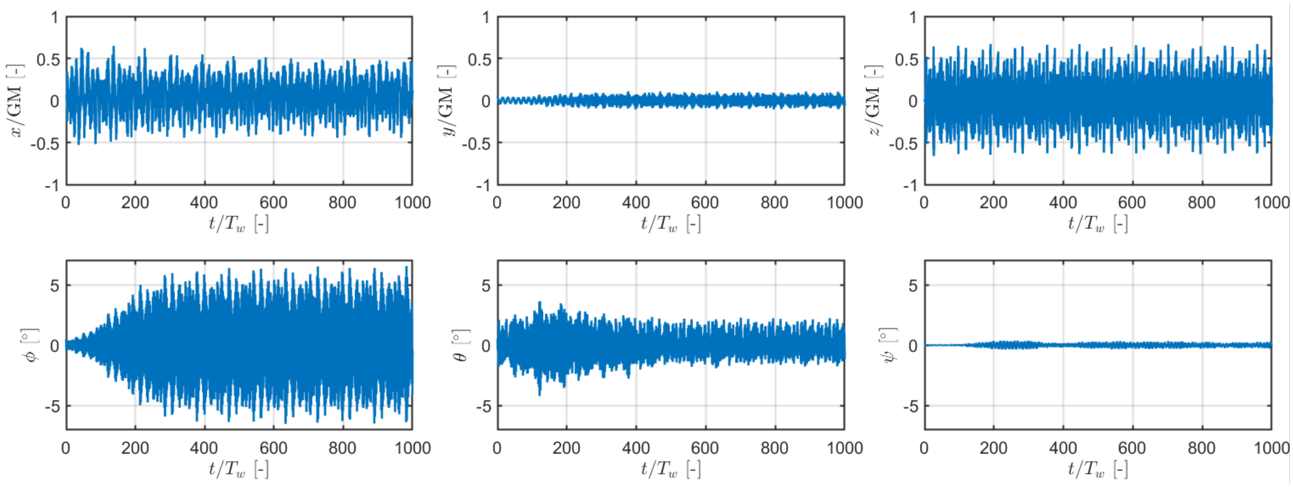

Figure 3: Dynamic response to a realization of a panchromatic wave with peak period $T_p = T_{n,5}/2$ and significant wave height $H_s = GM$.

if the mathematical model is coupled to a physical system). However, even with ideal inertial parameters, sustained bounded yaw response may be obtained if all other 5 DoFs are excited. This particular scenario arises due to parametric resonance conditions of the roll DoF, namely when the excitation force frequency is about twice the roll natural frequency. The proposed model, thanks to the nonlinear FK formulation, is also able to articulate parametric resonance.

Acknowledgement

This research has received funding from the European Research Council (ERC) under the European Union's Horizon 2020 research and innovation program under Grant No. 832140 and Grant No. 867453, and the Higher Education Excellence Program of the Ministry of Human Capacities in the frame of the Water Sciences & Disaster Prevention Research Area of BME (BME FIKP-VIZ), and in part by the National Research, Development and Innovation Fund through the Thematic Excellence Program under Grant TUDFO/51757/2019- ITM.

References

[1] J. N. Newman, L. Landweber, Marine Hydrodynamics, Vol. 45, The MIT Press, 1978. doi:10.1115/1.3424341.

[2] G. Giorgi, R. P. Gomes, J. C. Henriques, L. M. Gato, G. Bracco, G. Mattiazzo, Detecting parametric resonance in a floating oscillating water column device for wave energy conversion: Numerical simulations and validation with physical model tests, Applied Energy 276. doi:10.1016/j.apenergy.2020.115421.

[3] R. Genest, J. Davidson, J. V. Ringwood, Adaptive control of a wave energy converter, IEEE Transactions on Sustainable Energy 9 (4) (2018) 1588–1595.

[4] G. Bracco, M. Casassa, E. Giorcelli, G. Giorgi, M. Martini, G. Mattiazzo, B. Passione, M. Raffero, G. Vissio, Application of sub-optimal control techniques to a gyroscopic Wave Energy Converter, in: Renewable Energies Offshore, 2014, pp. 265–269.

[5] L. Genuardi, G. Bracco, S. A. Sirigu, M. Bonfanti, B. Paduano, P. Dafnakis, G. Mattiazzo, An application of model predictive control logic to inertial sea wave energy converter, in: Mechanisms and Machine Science, Vol. 73, Springer Netherlands, 2019, pp. 3561–3571. doi:10.1007/978-3-030-20131-9_351.

[6] N. Faedo, F. J. Dores Piuma, G. Giorgi, J. V. Ringwood, Nonlinear model reduction for wave energy systems: a moment-matching-based approach, Nonlinear Dynamics (2020) 1–23doi:10.1007/s11071-020-06028-0.

[7] A. S. Sirigu, F. Gallizio, G. Giorgi, M. Bonfanti, G. Bracco, G. Mattiazzo, Numerical and Experimental Identification of the Aerodynamic Power Losses of the ISWEC, Journal of Marine Science and Engineering 8 (49) (2020) 1–25. doi:10.3390/jmse8010049.

[8] M. Penalba, G. Giorgi, J. V. Ringwood, Mathematical modelling of wave energy converters: a review of nonlinear approaches, Renewable and Sustainable Energy Reviews 78 (2017) 1188–1207. doi:10.1016/j.rser.2016.11.137.

[9] J. Davidson, R. Costello, Efficient Nonlinear Hydrodynamic Models for Wave Energy Converter Design — A Scoping Study (2020) 1–65doi:10.3390/jmse8010035.

[10] F. Wendt, K. Nielsen, Y.-h. Yu, H. Bingham, C. Eskilsson, B. Kramer, A. Babarit, T. Bunnik, R. Costello, S. Crowley, G. Giorgi, S. Giorgi, S. Girardin, D. Greaves, Ocean Energy Systems wave energy modeling task : modeling , verification , and validation of wave energy converters, Journal of Marine Science and Engineering 7 (379) (2019) 1–22. doi:10.3390/jmse7110379.

[11] E. Ransley, S. Yan, S. Brown, D. Graham, P.-H. Musiedlak, C. Windt, J. Ringwood, J. Davidson, P. Schmitt, J. X. H. Wang, Q. Ma, Z. H. Xie, G. Giorgi, J. Hughes, A. Williams, I. Masters, Z. Lin, H. Chen, L. Qian, Z. Ma, D. Causon, C. Mingham, Q. Chen, H. Ding, J. Zang, J. van Rij, Y. Yu, N. Tom, Z. Li, B. Bouscasse, G. Ducrozet, H. Bingham, A blind comparative study of focused wave interactions with floating structures ({CCP-WSI Blind Test Series 3}), International Journal of Offshore and Polar Engineering 30 (1) (2020) 1–10. doi:10.17736/ijope.2020.jc774.

[12] M. Fontana, P. Casalone, S. A. Sirigu, G. Giorgi, Viscous Damping Identification for a Wave Energy Converter Using CFD-URANS Simulations, Journal of Marine Science and Engineering 8 (355) (2020) 1–26. doi:10.3390/jmse8050355.

[13] L. Letournel, C. Chauvigné, B. Gelly, A. Babarit, G. Ducrozet, P. Ferrant, Weakly nonlinear modeling of submerged wave energy converters, Applied Ocean Research 75 (March) (2018) 201–222. doi:10.1016/j.apor.2018.03.014.

[14] G. Giorgi, J. Davidson, G. Habib, G. Bracco, G. Mattiazzo, T. Kalmár-nagy, Nonlinear Dynamic and Kinematic Model of a Spar-Buoy : Parametric Resonance and Yaw Numerical Instability, Journal of Marine Science and Engineering 8 (504) (2020) 1–17. doi:10.3390/jmse8070504.

[15] S. H. Scott, D. A. Winter, Biomechanical model of the human foot: kinematics and kinetics during the stance phase of walking, Journal of biomechanics 26 (9) (1993) 1091–1104.

[16] U. H. Buzzi, N. Stergiou, M. J. Kurz, P. A. Hageman, J. Heidel, Nonlinear dynamics indicates aging affects variability during gait, Clinical biomechanics 18 (5) (2003) 435–443.

[17] A. J. Ijspeert, J. Nakanishi, S. Schaal, Movement imitation with nonlinear dynamical systems in humanoid robots, in: Proceedings 2002 IEEE International Conference on Robotics and Automation (Cat. No. 02CH37292), Vol. 2, IEEE, 2002, pp. 1398–1403.

[18] T. I. Fossen, S. I. Sagatun, Adaptive control of nonlinear systems: A case study of underwater robotic systems, Journal of Robotic Systems 8 (3) (1991) 393–412.

[19] T. D. Burton, A. M. Whitman, Nonlinear kinematics of wheel-rail contact.

[20] M. Kaminaga, M. Murata, Y. Tateishi, Factoring nonlinear kinematics into new suspension design: a CAE approach to vehicle roll dynamics, SAE transactions (1994) 1188–1198.

[21] H. J. Kim, D. H. Shim, S. Sastry, Nonlinear model predictive tracking control for rotorcraft-based unmanned aerial vehicles, in: Proceedings of the 2002 American Control Conference (IEEE Cat. No. CH37301), Vol. 5, IEEE, 2002, pp. 3576–3581.

[22] E. J. Clark, E. J. Griffith, S. Maskell, J. F. Ralph, Nonlinear kinematics for improved helicopter tracking, in: 2017 20th International Conference on Information Fusion (Fusion), IEEE, 2017, pp. 1–6.

[23] G. Naganathan, A. H. Soni, Coupling effects of kinematics and flexibility in manipulators, The International journal of robotics research 6 (1) (1987) 75–84.

[24] G. Naganathan, A. H. Soni, Nonlinear modeling of kinematic and flexibility effects in manipulator design, Journal of Mechanical Design.

[25] A. Babarit, J. H. Todalshaug, A. Kurniawan, M. Muliawan, T. Moan, J. Krokstad, The NumWEC Project: Numerical Esitmation of Energy Delivery from a Selection of Wave Energy Converters (December) (2011) 1–317. doi:10.13140/RG.2.1.3807.8885.

[26] J. Orszaghova, H. Wolgamot, S. Draper, P. H. Taylor, A. Rafiee, Onset and limiting amplitude of yaw instability of a submerged three-tethered buoy, Proceedings of the Royal Society A: Mathematical, Physical and Engineering Sciencesdoi:10.1098/rspa.2019.0762.

[27] H. Wang, A. Somayajula, J. Falzarano, Z. Xie, Development of a Blended Time-Domain Program for Predicting the Motions of a Wave Energy Structure, Journal of Marine Science and Engineering 8 (1) (2019) 1. doi:10.3390/jmse8010001.

[28] G. Giorgi, N. Faedo, Performance enhancement of a vibration energy harvester via harmonic time-varying damping: A pseudospectral-based approach, Mechanical Systems and Signal Processing 165 (2022) 108331. doi:10.1016/J.YMSSP.2021.108331.

[29] G. Giorgi, Parametric resonance exploitation due to periodic damping in an electromechanical energy harvester, International Journal of Mechanics and Control 22 (2021) 77–85.

[30] G. Giorgi, R. P. F. Gomes, G. Bracco, G. Mattiazzo, The effect of mooring line parameters in inducing parametric resonance on the Spar-buoy oscillating water column wave energy converter, Journal of Marine Science and Engineering 8 (1) (2020) 1–20. doi:10.3390/JMSE8010029.

[31] G. Giorgi, R. P. F. Gomes, G. Bracco, G. Mattiazzo, Numerical investigation of parametric resonance due to hydrodynamic coupling in a realistic wave energy converter, Nonlinear Dynamicsdoi:10.1007/s11071-020-05739-8.

[32] G. Giorgi, S. Sirigu, M. Bonfanti, G. Bracco, G. Mattiazzo, Fast nonlinear froude–krylov force calculation for prismatic floating platforms: a wave energy conversion application case, Journal of Ocean Engineering and Marine Energy 2021 7 (2021) 439–457. doi:10.1007/S40722-021-00212-Z.

[33] G. Giorgi, Nonlinear Froude-Krylov Matlab demonstration toolbox (2019). doi:10.5281/zenodo.4065202.

[34] T. I. Fossen, H. Nijmeijer, Parametric resonance in dynamical systems, Springer, 2012. doi:10.1007/978-1-4614-1043-0.

[35] J. Davidson, J. V. Ringwood, Mathematical modelling of mooring systems for wave energy converters - A review, Energies 10 (5). doi:10.3390/en10050666.

[36] B. Paduano, G. Giorgi, R. P. F. Gomes, E. Pasta, J. C. C. Henriques, L. M. C. Gato, G. Mattiazzo, Experimental Validation and Comparison of Numerical Models for the Mooring System of a Floating Wave Energy Converter, Journal of Marine Science and Engineering 8 (8) (2020) 565. doi:10.3390/jmse8080565.

[37] M. Bonfanti, G. Bracco, P. Dafnakis, E. Giorcelli, B. Passione, N. Pozzi, S. Sirigu, G. Mattiazzo, Application of a passive control technique to the ISWEC: Experimental tests on a 1:8 test rig, in: NAV International Conference on Ship and Shipping Research, no. 221499, 2018, pp. 60–70. doi:10.3233/978-1-61499-870-9-60.

[38] S. A. Sirigu, G. Bracco, M. Bonfanti, P. Dafnakis, G. Mattiazzo, On-board sea state estimation method validation based on measured floater motion, IFAC-PapersOnLine 51 (29) (2018) 68–73. doi:10.1016/J.IFACOL.2018.09.471.

[39] K. R. Tarrant, C. Meskell, Investigation on parametrically excited motions of point absorbers in regular waves, Ocean Engineering 111 (2016) 67–81. doi:10.1016/j.oceaneng.2015.10.041.

[40] G. Giorgi, J. V. Ringwood, Parametric motion detection for an oscillating water column spar buoy., in: Proceedings of the 3rd International Conference on Renewable Energies Offshore RENEW, Lisbon, 2018.

[41] Z. Jingrui, T. Yougang, S. Wenjun, A study on the combination resonance response of a classic spar platform, JVC/Journal of Vibration and Control 16 (14) (2010) 2083–2107. doi:10.1177/1077546309349393.

[42] E. Gavassoni, P. B. Gonçalves, D. M. Roehl, Nonlinear vibration modes and instability of a conceptual model of a spar platform, Nonlinear Dynamics 76 (1) (2014) 809–826. doi:10.1007/s11071-013-1171-6.

[43] R. Gomes, J. Henriques, L. Gato, A. Falcão, Time-domain simulation of a slack-moored floating oscillating water column and validation with physical model tests, Renewable Energy 149 (2020) 165–180. doi:10.1016/J.RENENE.2019.11.159.